

Multiboson Hanbury Brown-Twiss correlations for partially coherent sources in relativistic heavy-ion collisions in a multiphase transport model

Shi-Yao Wang¹, Jun-Ting Ye¹, Wei-Ning Zhang^{1,2*}

¹*School of Physics, Dalian University of Technology, Dalian, Liaoning 116024, China*

²*School of Physics, Harbin Institute of Technology,
Harbin, Heilongjiang 150006, China*

Abstract

We use a multi-phase transport (AMPT) model to study multi-pion and multi-kaon Hanbury Brown-Twiss (HBT) correlations for the partially coherent particle-emitting sources in relativistic heavy-ion collisions. A density-dependent longitudinal coherent emission length and density-dependent transverse coherent emission length are introduced in calculating the multi-boson HBT correlation functions of the partially coherent sources. We compare the model results of three- and four-pion HBT correlation functions with experimental data in Pb-Pb collisions at center-of-mass energy $\sqrt{s_{NN}}=2.76$ TeV, and investigate the influences of boson coherent emissions on the multi-pion and multi-kaon correlation functions. We find that all of the three- and four-pion correlation functions of the partially coherent sources are consistent with experimental data. Coherent emission leads to the intercept decreases of the multi-boson correlation functions. The intercepts of the multi-kaon correlation functions of the partially coherent source are higher than those of the multi-pion correlation functions, because low kaon densities lead to smaller kaon coherent emission lengths than pion emission lengths. The intercepts of multi-boson correlation functions of partially coherent sources in high transverse momentum intervals are higher than those in low transverse momentum intervals because particle de Broglie wavelengths are small at high momenta.

Keywords: multi-boson HBT correlations, partially coherent sources, AMPT model, relativistic heavy ion collisions

PACS numbers: 25.75.Gz, 25.75.-q, 21.65.jk

* wnzhang@dlut.edu.cn

I. INTRODUCTION

Identical boson Hanbury Brown-Twiss (HBT) correlations are important observables in high-energy heavy-ion collisions [1–6]. At the Large Hadron Collider (LHC), the multiplicities of identical bosons in an event are high in nucleus-nucleus collisions, e.g., several thousands for pions and several hundreds for kaons [7]. So, the study of multi-boson HBT correlations becomes possible [8–14]. Pions are the most abundant boson produced in high-energy nucleus-nucleus collisions. The observed suppressions of two- and multi-pion HBT correlation functions at small relative momenta in experiments may indicate that the pion-emitting sources are partially coherent [1–6, 8–19].

Compared with two-pion HBT correlations, multi-pion HBT correlations are sensitive to the source coherence [11–14, 20–22]. In this paper, we study the pion and kaon three- and four-particle HBT correlations for partially coherent sources in Pb-Pb central collisions at $\sqrt{s_{NN}}=2.76$ TeV, using a multi-phase transport model (AMPT) [23, 24]. We construct the partially coherent sources for pion and kaon emissions with a consistent longitudinal coherent emission length and a transverse coherent emission length, which are dependent on the particle de Broglie wavelengths [25], as well as the boson densities at generation configurations in the AMPT model. It is found that both of the three- and four-pion correlation functions of the partially coherent sources calculated in the AMPT model are consistent with the experimental results in Pb-Pb collisions at $\sqrt{s_{NN}}=2.76$ TeV at the LHC [10]. The intercepts of the multi-boson correlation functions of partially coherent sources reflect the influences of boson coherent emission on the correlation functions. We find that the intercepts of the multi-kaon correlation functions of partially coherent sources are higher than those of multi-pion correlation functions, and the intercepts of the multi-boson correlation functions in high transverse momentum intervals are higher than those in low transverse momentum intervals.

The rest of this paper is organized as follows. In Section II, we introduce the consistent boson density dependent coherent emission lengths for the pion and kaon partially coherent sources, and describe the calculation of the multi-boson HBT correlation functions in the AMPT model. Section III presents the results of pion and kaon multi-particle HBT correlation functions in Pb-Pb central collisions at $\sqrt{s_{NN}}=2.76$ TeV in the AMPT model, and compares the model results of three- and four-pion correlation functions with experimental

data. We also calculate the intercepts of the multi-boson correlation functions of the partially coherent sources, and investigate the influences on them of boson coherent emission. We summarize this work and present conclusions in Section IV.

II. MULTIBOSON HBT CORRELATIONS FOR PARTIALLY COHERENT SOURCES IN THE AMPT MODEL

A. Multiboson HBT correlation functions

The HBT correlation functions of $m (\geq 2)$ bosons are defined as

$$C_m(\mathbf{p}_1, \mathbf{p}_2, \dots, \mathbf{p}_m) = \frac{P_m(\mathbf{p}_1, \mathbf{p}_2, \dots, \mathbf{p}_m)}{P_1(\mathbf{p}_1)P_1(\mathbf{p}_2) \cdots P_1(\mathbf{p}_m)}, \quad (1)$$

where $P_1(\mathbf{p}_i)$ ($i = 1, 2, \dots, m$) is the distribution of single-boson momentum \mathbf{p}_i , and $P_m(\mathbf{p}_1, \mathbf{p}_2, \dots, \mathbf{p}_m)$ is the m identical boson momentum distribution in an event.

Considering the bosons emitted from completely chaotic sources and with small momentum differences, we can write the denominator and numerator, respectively, in Eq. (1) in the smoothed approximation as [25]

$$P_1(\mathbf{p}_1)P_1(\mathbf{p}_2) \cdots P_1(\mathbf{p}_m) = \sum_{X_1} \sum_{X_2} \cdots \sum_{X_m} A^2(\mathbf{p}_1, X_1) A^2(\mathbf{p}_2, X_2) \cdots A^2(\mathbf{p}_m, X_m), \quad (2)$$

$$\begin{aligned} P_m(\mathbf{p}_1, \mathbf{p}_2, \dots, \mathbf{p}_m) &= \sum_{X_1} \sum_{X_2} \cdots \sum_{X_m} A^2(\mathbf{p}_1, X_1) A^2(\mathbf{p}_2, X_2) \cdots A^2(\mathbf{p}_m, X_m) \\ &\quad \times \left| \Psi(\mathbf{p}_1, \mathbf{p}_2, \dots, \mathbf{p}_m; X_1, X_2, \dots, X_m) \right|^2, \end{aligned} \quad (3)$$

where $A(\mathbf{p}_i, X_i)$ is the magnitude of the amplitude for emitting a pion with momentum \mathbf{p}_i at four-coordinate X_i (freeze-out coordinates), and

$$\Psi(\mathbf{p}_1, \mathbf{p}_2, \dots, \mathbf{p}_m; X_1, X_2, \dots, X_m) = \frac{1}{\sqrt{m!}} \sum_{\sigma} \sum_{j=1}^m e^{ip_j \cdot X_{\sigma(j)}}, \quad (4)$$

where p_j is the four-momentum for \mathbf{p}_j , $\sigma(j)$ is the j th element of a permutation of the sequence $\{1, 2, \dots, m\}$, and \sum_{σ} denotes summation over all $m!$ permutations of the sequence.

For $m = 2, 3$, and 4 , respectively, we have

$$C_2(\mathbf{p}_1, \mathbf{p}_2) = \sum_{X_1} \sum_{X_2} A^2(\mathbf{p}_1, X_1) A^2(\mathbf{p}_2, X_2) \left\{ 1 + \text{Re} [f(p_1 - p_2, X_1) f^*(p_1 - p_2, X_2)] \right\}$$

$$\begin{aligned}
& \left/ \sum_{X_1} \sum_{X_2} A^2(\mathbf{p}_1, X_1) A^2(\mathbf{p}_2, X_2) \right. \\
&= \sum_{X_1} \sum_{X_2} A^2(\mathbf{p}_1, X_1) A^2(\mathbf{p}_2, X_2) \left\{ 1 + \cos [(p_1 - p_2) \cdot (X_1 - X_2)] \right\} \\
& \left/ \sum_{X_1} \sum_{X_2} A^2(\mathbf{p}_1, X_1) A^2(\mathbf{p}_2, X_2), \right. \tag{5}
\end{aligned}$$

$$\begin{aligned}
C_3(\mathbf{p}_1, \mathbf{p}_2, \mathbf{p}_3) &= \sum_{X_1} \sum_{X_2} \sum_{X_3} A^2(\mathbf{p}_1, X_1) A^2(\mathbf{p}_2, X_2) A^2(\mathbf{p}_3, X_3) \\
&\times \left\{ 1 + \text{Re}[f(p_1 - p_2, X_1) f^*(p_1 - p_2, X_2)] + \text{Re}[f(p_1 - p_3, X_1) f^*(p_1 - p_3, X_3)] \right. \\
&\quad + \text{Re}[f(p_2 - p_3, X_2) f^*(p_2 - p_3, X_3)] \\
&\quad \left. + 2\text{Re}[f(p_1 - p_2, X_1) f(p_2 - p_3, X_2) f(p_3 - p_1, X_3)] \right\} \\
& \left/ \sum_{X_1} \sum_{X_2} \sum_{X_3} A^2(\mathbf{p}_1, X_1) A^2(\mathbf{p}_2, X_2) A^2(\mathbf{p}_3, X_3), \right. \tag{6}
\end{aligned}$$

$$\begin{aligned}
C_4(\mathbf{p}_1, \mathbf{p}_2, \mathbf{p}_3, \mathbf{p}_4) &= \sum_{X_1} \sum_{X_2} \sum_{X_3} \sum_{X_4} A^2(\mathbf{p}_1, X_1) A^2(\mathbf{p}_2, X_2) A^2(\mathbf{p}_3, X_3) A^2(\mathbf{p}_4, X_4) \\
&\times \left\{ 1 + \text{Re}[f(p_1 - p_2, X_1) f^*(p_1 - p_2, X_2)] + \text{Re}[f(p_1 - p_3, X_1) f^*(p_1 - p_3, X_3)] \right. \\
&\quad + \text{Re}[f(p_1 - p_4, X_1) f^*(p_1 - p_4, X_4)] + \text{Re}[f(p_2 - p_3, X_2) f^*(p_2 - p_3, X_3)] \\
&\quad + \text{Re}[f(p_2 - p_4, X_2) f^*(p_2 - p_4, X_4)] + \text{Re}[f(p_3 - p_4, X_3) f^*(p_3 - p_4, X_4)] \\
&\quad + 2\text{Re}[f(p_1 - p_2, X_1) f(p_2 - p_3, X_2) f(p_3 - p_1, X_3)] \\
&\quad + 2\text{Re}[f(p_1 - p_2, X_1) f(p_2 - p_4, X_2) f(p_4 - p_1, X_4)] \\
&\quad + 2\text{Re}[f(p_1 - p_3, X_1) f(p_3 - p_4, X_3) f(p_4 - p_1, X_4)] \\
&\quad + 2\text{Re}[f(p_2 - p_3, X_2) f(p_3 - p_4, X_3) f(p_4 - p_2, X_4)] \\
&\quad + \text{Re}[f(p_1 - p_2, X_1) f^*(p_1 - p_2, X_2)] \text{Re}[f(p_3 - p_4, X_3) f^*(p_3 - p_4, X_4)] \\
&\quad + \text{Re}[f(p_1 - p_3, X_1) f^*(p_1 - p_3, X_3)] \text{Re}[f(p_2 - p_4, X_2) f^*(p_2 - p_4, X_4)] \\
&\quad + \text{Re}[f(p_1 - p_4, X_1) f^*(p_1 - p_4, X_4)] \text{Re}[f(p_2 - p_4, X_2) f^*(p_2 - p_3, X_3)] \\
&\quad + 2\text{Re}[f(p_1 - p_2, X_1) f(p_2 - p_3, X_2) f(p_3 - p_4, X_3) f(p_4 - p_1, X_4)] \\
&\quad + 2\text{Re}[f(p_1 - p_2, X_1) f(p_2 - p_4, X_2) f(p_4 - p_3, X_4) f(p_3 - p_1, X_3)] \\
&\quad \left. + 2\text{Re}[f(p_1 - p_3, X_1) f(p_3 - p_2, X_3) f(p_2 - p_4, X_2) f(p_4 - p_1, X_4)] \right\} \\
& \left/ \sum_{X_1} \sum_{X_2} \sum_{X_3} \sum_{X_4} A^2(\mathbf{p}_1, X_1) A^2(\mathbf{p}_2, X_2) A^2(\mathbf{p}_3, X_3) A^2(\mathbf{p}_4, X_4), \right. \tag{7}
\end{aligned}$$

where

$$f(p_i - p_j, X) = e^{i(p_i - p_j) \cdot X} = f^*(p_j - p_i, X), \quad i, j = 1, 2, 3, 4, i \neq j, \tag{8}$$

is called the amplitude of the correlator between the i th and j th bosons.

In Eq. (6) the last term in curly braces expresses the pure triplet correlation of the three bosons. The three-boson cumulant correlation function is defined as

$$c_3(\mathbf{p}_1, \mathbf{p}_2, \mathbf{p}_3) = \sum_{X_1} \sum_{X_2} \sum_{X_3} A^2(\mathbf{p}_1, X_1) A^2(\mathbf{p}_2, X_2) A^2(\mathbf{p}_3, X_3) \\ \times \left\{ 1 + 2\text{Re}[f(p_1 - p_2, X_1) f(p_2 - p_3, X_2) f(p_3 - p_1, X_1)] \right\} \\ \bigg/ \sum_{X_1} \sum_{X_2} \sum_{X_3} A^2(\mathbf{p}_1, X_1) A^2(\mathbf{p}_2, X_2) A^2(\mathbf{p}_3, X_3). \quad (9)$$

In Eq. (7), the eighth through eleventh terms in curly braces express the pure triplet correlations of the three bosons, the twelfth through fourteenth terms in curly braces express the correlations of the double boson pairs, and the last three terms in curly brackets express the pure quadruplet correlations of the four bosons. The four-boson cumulant correlation functions c_4 , a_4 , and b_4 are defined respectively as [10, 12]

$$c_4(\mathbf{p}_1, \mathbf{p}_2, \mathbf{p}_3, \mathbf{p}_4) = \sum_{X_1} \sum_{X_2} \sum_{X_3} \sum_{X_4} A^2(\mathbf{p}_1, X_1) A^2(\mathbf{p}_2, X_2) A^2(\mathbf{p}_3, X_3) A^2(\mathbf{p}_4, X_4) \\ \times \left\{ 1 + 2\text{Re}[f(p_1 - p_2, X_1) f(p_2 - p_3, X_2) f(p_3 - p_4, X_3) f(p_4 - p_1, X_4)] \right. \\ \left. + 2\text{Re}[f(p_1 - p_2, X_1) f(p_2 - p_4, X_2) f(p_4 - p_3, X_4) f(p_3 - p_1, X_3)] \right. \\ \left. + 2\text{Re}[f(p_1 - p_3, X_1) f(p_3 - p_2, X_3) f(p_2 - p_4, X_2) f(p_4 - p_1, X_4)] \right\} \\ \bigg/ \sum_{X_1} \sum_{X_2} \sum_{X_3} \sum_{X_4} A^2(\mathbf{p}_1, X_1) A^2(\mathbf{p}_2, X_2) A^2(\mathbf{p}_3, X_3) A^2(\mathbf{p}_4, X_4), \quad (10)$$

$$a_4(\mathbf{p}_1, \mathbf{p}_2, \mathbf{p}_3, \mathbf{p}_4) = \sum_{X_1} \sum_{X_2} \sum_{X_3} \sum_{X_4} A^2(\mathbf{p}_1, X_1) A^2(\mathbf{p}_2, X_2) A^2(\mathbf{p}_3, X_3) A^2(\mathbf{p}_4, X_4) \\ \times \left\{ 1 + 2\text{Re}[f(p_1 - p_2, X_1) f(p_2 - p_3, X_2) f(p_3 - p_1, X_3)] \right. \\ \left. + 2\text{Re}[f(p_1 - p_2, X_1) f(p_2 - p_4, X_2) f(p_4 - p_1, X_4)] \right. \\ \left. + 2\text{Re}[f(p_1 - p_3, X_1) f(p_3 - p_4, X_3) f(p_4 - p_1, X_1)] \right. \\ \left. + 2\text{Re}[f(p_2 - p_3, X_2) f(p_3 - p_4, X_3) f(p_4 - p_2, X_4)] \right. \\ \left. + \text{Re}[f(p_1 - p_2, X_1) f^*(p_1 - p_2, X_2)] \text{Re}[f(p_3 - p_4, X_3) f^*(p_3 - p_4, X_4)] \right. \\ \left. + \text{Re}[f(p_1 - p_3, X_1) f^*(p_1 - p_3, X_3)] \text{Re}[f(p_2 - p_4, X_2) f^*(p_2 - p_4, X_4)] \right. \\ \left. + \text{Re}[f(p_1 - p_4, X_1) f^*(p_1 - p_4, X_4)] \text{Re}[f(p_2 - p_4, X_2) f^*(p_2 - p_3, X_3)] \right. \\ \left. + 2\text{Re}[f(p_1 - p_2, X_1) f(p_2 - p_3, X_2) f(p_3 - p_4, X_3) f(p_4 - p_1, X_4)] \right. \\ \left. + 2\text{Re}[f(p_1 - p_2, X_1) f(p_2 - p_4, X_2) f(p_4 - p_3, X_4) f(p_3 - p_1, X_3)] \right. \\ \left. + 2\text{Re}[f(p_1 - p_3, X_1) f(p_3 - p_2, X_3) f(p_2 - p_4, X_2) f(p_4 - p_1, X_4)] \right\}$$

$$\bigg/ \sum_{X_1} \sum_{X_2} \sum_{X_3} \sum_{X_4} A^2(\mathbf{p}_1, X_1) A^2(\mathbf{p}_2, X_2) A^2(\mathbf{p}_3, X_3) A^2(\mathbf{p}_4, X_4), \quad (11)$$

and

$$\begin{aligned} b_4(\mathbf{p}_1, \mathbf{p}_2, \mathbf{p}_3, \mathbf{p}_4) = & \sum_{X_1} \sum_{X_2} \sum_{X_3} \sum_{X_4} A^2(\mathbf{p}_1, X_1) A^2(\mathbf{p}_2, X_2) A^2(\mathbf{p}_3, X_3) A^2(\mathbf{p}_4, X_4) \\ & \times \left\{ 1 + 2\text{Re}[f(p_1 - p_2, X_1) f(p_2 - p_3, X_2) f(p_3 - p_1, X_3)] \right. \\ & + 2\text{Re}[f(p_1 - p_2, X_1) f(p_2 - p_4, X_2) f(p_4 - p_1, X_4)] \\ & + 2\text{Re}[f(p_1 - p_3, X_1) f(p_3 - p_4, X_3) f(p_4 - p_1, X_1)] \\ & + 2\text{Re}[f(p_2 - p_3, X_2) f(p_3 - p_4, X_3) f(p_4 - p_2, X_4)] \\ & + 2\text{Re}[f(p_1 - p_2, X_1) f(p_2 - p_3, X_2) f(p_3 - p_4, X_3) f(p_4 - p_1, X_4)] \\ & + 2\text{Re}[f(p_1 - p_2, X_1) f(p_2 - p_4, X_2) f(p_4 - p_3, X_4) f(p_3 - p_1, X_3)] \\ & \left. + 2\text{Re}[f(p_1 - p_3, X_1) f(p_3 - p_2, X_3) f(p_2 - p_4, X_2) f(p_4 - p_1, X_4)] \right\} \\ & \bigg/ \sum_{X_1} \sum_{X_2} \sum_{X_3} \sum_{X_4} A^2(\mathbf{p}_1, X_1) A^2(\mathbf{p}_2, X_2) A^2(\mathbf{p}_3, X_3) A^2(\mathbf{p}_4, X_4). \end{aligned} \quad (12)$$

B. Calculation of multi-boson correlation functions in the AMPT model

The AMPT model has been successfully used to describe the observables in high-energy heavy-ion collisions [23–41]. It is a hybrid composed of initialization, parton transport, hadronization, and hadron transport [24]. The initialization of collisions in the AMPT model is performed using the HIJING model [42]. The parton and hadron transport are described by the ZPC (Zhang’s parton cascade) model [43] and ART model [44], respectively. In this study, we investigate the multi-boson correlations of identical pions and kaons generated with the string melting version of the AMPT model [23, 24], for Pb-Pb central collisions at $\sqrt{s_{NN}} = 2.76$ TeV. The impact parameter b is taken between 0 and 3.5 fm for centrality 0–5% [45], and the freeze-out times of the pion and kaon sources are taken to be 40 fm/c. We take the model parameter μ of parton screening mass to be 2.2814 fm^{-1} [24] in the calculations. The strong coupling constant α_s is taken to be 0.47, corresponding to a parton-scattering cross section of 6 mb [24].

With the AMPT model, one can trace back to the origin of a freeze-out particle, its generation coordinate $\mathbf{r} = (x, y, z) = (\mathbf{r}_T, z)$, momentum $\mathbf{k} = (\mathbf{k}_T, k_Z)$, and parent. We previously calculated the two-pion HBT correlation functions for the partially coherent sources in the AMPT model [25]. It was assumed that the emissions of two pions are coherent

if their longitudinal difference of generation coordinates $\Delta z = |z_1 - z_2|$ is smaller than the longitudinal coherent emission length $L_{CZ}(k_{1Z}, k_{2Z})$ and their transverse difference of generation coordinates $\Delta r_T = \sqrt{(x_1 - x_2)^2 + (y_1 - y_2)^2}$ is smaller than the transverse coherent emission length $L_{CT}(k_{1T}, k_{2T})$. In this case, the contribution of this pair to the two-pion correlator in Eq. (5) is zero. In the calculations of multi-boson HBT correlation functions for the partially coherent sources in the AMPT model, we substitute the factor $f(\mathbf{p}_i - \mathbf{p}_j, X)$ ($i, j = 1, 2, 3, 4, i \neq j$) in Eqs. (6)–(10) with $F(\mathbf{p}_i - \mathbf{p}_j, X)$, and assume

$$\begin{aligned} F(\mathbf{p}_i - \mathbf{p}_j, X) &= 0, & \text{for } \Delta z_{ij} < L_{ijCZ} \text{ and } \Delta r_{ijT} < L_{ijCT}, \\ F(\mathbf{p}_i - \mathbf{p}_j, X) &= f(\mathbf{p}_i - \mathbf{p}_j, X), & \text{otherwise,} \end{aligned} \quad (13)$$

where $\Delta z_{ij} = |z_i - z_j|$, $\Delta r_{ijT} = \sqrt{(x_i - x_j)^2 + (y_i - y_j)^2}$, $i, j = 1, 2, 3, 4, i \neq j$, and L_{ijCZ} and L_{ijCT} are the respective longitudinal and transverse coherent emission lengths.

In our previous work [25], the coherent emission lengths are proportional to the de Broglie wavelengths of the two pions, in which case the proportionality coefficients should differ for different kinds of bosons, which are produced at different evolution stages of the collision systems and have different multiplicities. For identical bosons emitted from a source with finite size, the emission coherence is not only related to the bosons de Broglie wavelengths ($\sim h/k$) but also their density in the source. Considering that the emission coherence is related to the boson density as well as the de Broglie wavelengths of the two bosons, we extend the longitudinal and transverse coherent emission lengths in Ref. [25] as

$$L_{ijCZ} = a'_Z \langle D_Z \rangle \left[\frac{h}{k_{iZ}} + \frac{h}{k_{jZ}} \right], \quad (14)$$

and

$$L_{ijCT} = a'_T \langle D_T \rangle \left[\frac{h}{k_{iT}} + \frac{h}{k_{jT}} \right], \quad (15)$$

where $i, j = 1, 2, 3, 4, i \neq j$; a'_Z and a'_T are longitudinal and transverse parameters, respectively, which are universal constants for the collision system and can be determined by comparing the model HBT results with experimental data; k_{iZ} and k_{iT} are the respective boson longitudinal and transverse generation momenta. Because the source properties in longitudinal and transverse directions are much different in relativistic heavy-ion collisions, we introduced two independent coherent emission lengths in longitudinal and transverse directions in Ref. [25], which have different influences on the longitudinal and transverse HBT radii, to approach the two-pion HBT results in the AMPT model with the experimental

data [10]. In this paper, we assume that $\langle D_Z \rangle$ and $\langle D_T \rangle$ in Eqs. (14) and (15) are the boson densities related to the longitudinal and transverse coordinates, respectively,

$$\langle D_Z \rangle = \frac{M_b}{\langle r_Z \rangle}, \quad \langle D_T \rangle = \frac{M_b}{\pi \langle r_T \rangle^2}, \quad (16)$$

where M_b is the boson multiplicity, and $\langle r_Z \rangle$ and $\langle r_T \rangle$ are the respective averages of boson generation coordinates $r_Z = |z|$ and $r_T = \sqrt{x^2 + y^2}$ in the longitudinal and transverse directions.

Table I presents the identical pion and kaon densities $\langle D_Z \rangle$ and $\langle D_T \rangle$ in Pb-Pb central collisions ($0 < b < 3.5$ fm) at $\sqrt{s_{NN}} = 2.76$ TeV in transverse momentum intervals $0 < k_T < 0.4$ GeV/c, $0.4 < k_T < 1.0$ GeV/c, and $0 < k_T < 1.0$ GeV/c, calculated with 10^3 events in the AMPT model.

TABLE I: Identical pion and kaon densities $\langle D_Z \rangle$ and $\langle D_T \rangle$ in Pb-Pb central collisions at $\sqrt{s_{NN}} = 2.76$ TeV in different transverse momentum intervals, calculated in the AMPT model.

Pb-Pb@2.76 TeV	$0 < k_T < 0.4$ GeV/c	$0.4 < k_T < 1.0$ GeV/c	$0 < k_T < 1.0$ GeV/c
π , $\langle D_Z \rangle$ [fm ⁻¹]	213.744	286.782	248.840
π , $\langle D_T \rangle$ [fm ⁻²]	4.126	3.408	3.703
K, $\langle D_Z \rangle$ [fm ⁻¹]	68.261	70.771	70.287
K, $\langle D_T \rangle$ [fm ⁻²]	1.770	0.912	1.017

It can be seen that the boson longitudinal densities in the higher transverse momentum interval are greater than those in the lower transverse momentum interval and the boson transverse densities in the higher transverse momentum interval are smaller than those in the lower transverse momentum interval. It is because the average longitudinal coordinates in the higher transverse momentum interval are smaller than those in the low transverse momentum interval and the average transverse coordinates in the higher transverse momentum interval are greater than those in the low transverse momentum interval. In our calculations of multi-boson HBT correlations, we take the density values in the interval $0 < k_T < 1.0$ GeV/c, which covers almost all generated pions and kaons (99.9% for pion and 99.8% for kaon).

III. RESULTS OF MULTIBOSON HBT CORRELATION FUNCTIONS

We investigate multi-boson HBT correlations as functions of the three- and four-boson relative momentum variables [10–12]

$$Q_3 = \sqrt{Q_{12}^2 + Q_{23}^2 + Q_{13}^2} \quad (17)$$

and

$$Q_4 = \sqrt{Q_{12}^2 + Q_{13}^2 + Q_{14}^2 + Q_{23}^2 + Q_{24}^2 + Q_{34}^2}, \quad (18)$$

where $Q_{ij} = \sqrt{-(p_i - p_j)^\mu (p_i - p_j)_\mu}$ ($i, j = 1, 2, 3, 4$) is the invariant relative momentum of the boson pair. We investigate the multi-boson correlation functions in different intervals of the transverse momenta,

$$K_{T3} = \frac{|\mathbf{p}_{1T} + \mathbf{p}_{2T} + \mathbf{p}_{3T}|}{3} \quad (19)$$

and

$$K_{T4} = \frac{|\mathbf{p}_{1T} + \mathbf{p}_{2T} + \mathbf{p}_{3T} + \mathbf{p}_{4T}|}{4}. \quad (20)$$

A. Multi-pion correlation functions

Figure 1 shows the three-pion correlation functions $C_3(Q_3)$ and $c_3(Q_3)$ in Pb-Pb central collisions at $\sqrt{s_{NN}} = 2.76$ TeV, in the low and high transverse momentum intervals $0.16 < K_{T3} < 0.3$ GeV/ c and $0.3 < K_{T3} < 1$ GeV/ c , respectively. Here, the triangle and circle symbols refer to completely chaotic and partially coherent sources, respectively, in the AMPT model with impact parameter between 0 and 3.5 fm. Solid circles denote experimental data with centrality 0–5% [10]. In the model calculations for the partially coherent sources, we take the longitudinal and transverse parameters a'_Z and a'_T in Eqs. (14) and (15) to be 0.0031 fm and 0.662 fm², respectively, which are determined by comparing the model results with the experimental data [10]. The values of densities $\langle D_Z \rangle$ and $\langle D_T \rangle$ are taken to be those in the momentum interval $0 < k_T < 1.0$ GeV/ c in Table I. The values of $a'_Z \langle D_Z \rangle$ and $a'_T \langle D_T \rangle$ are consistent approximately with the corresponding parameters a_Z and a_T in our previous work [25], which investigated the two-pion HBT radii as functions of pair momentum for the chaotic and partially coherent sources in the AMPT model in Pb-Pb collisions at $\sqrt{s_{NN}} = 2.76$ TeV and compared them with the ALICE experimental data [10]. To compare the multi-pion correlation functions with experimental data, we take the pseudorapidity and

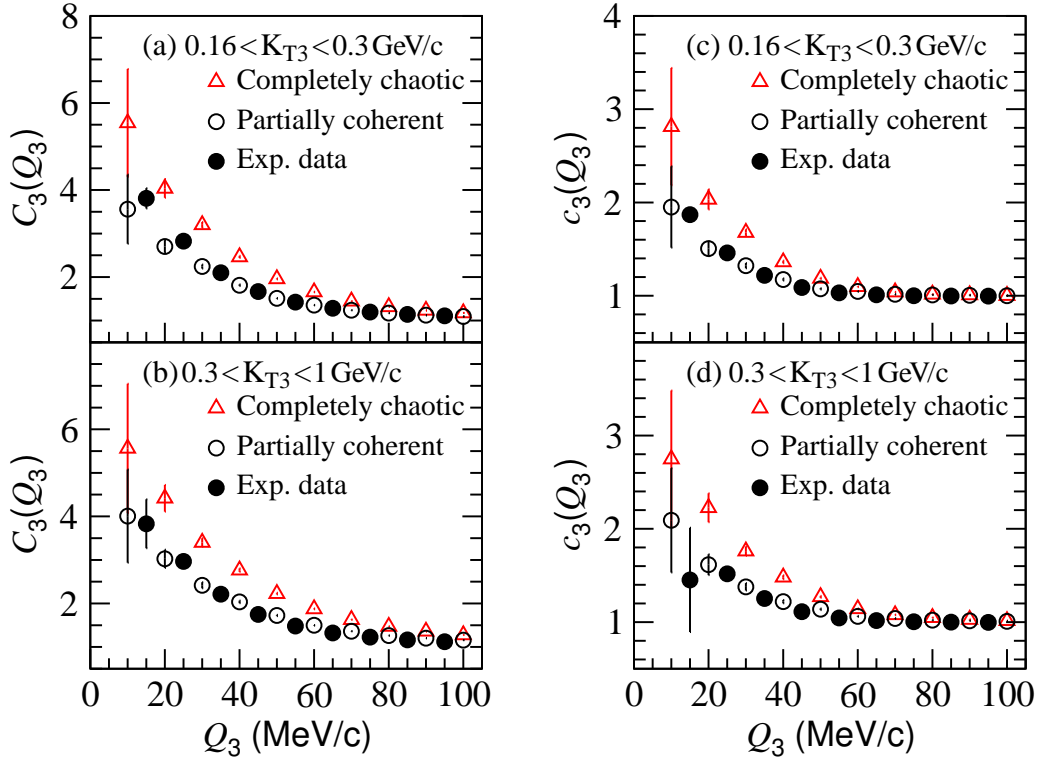


FIG. 1: (Color online) Three-pion correlation functions $C_3(Q_3)$ and $c_3(Q_3)$ for completely chaotic sources and partially coherent sources, respectively, in Pb-Pb central collisions at $\sqrt{s_{NN}} = 2.76$ TeV, calculated with the AMPT model. Experimental data [10] are plotted for comparison. Results in transverse momentum intervals $0.16 < K_{T3} < 0.3 \text{ GeV}/c$ and $0.3 < K_{T3} < 1 \text{ GeV}/c$ are shown in upper and lower panels, respectively.

transverse momentum cuts $|\eta| < 0.8$ and $0.16 < p_T < 1.0 \text{ GeV}/c$ [10] for pions in the AMPT model. The total number of model events is 6×10^3 .

Figure 2 shows the four-pion correlation functions $C_4(Q_4)$ and $c_4(Q_4)$ in Pb-Pb central collisions at $\sqrt{s_{NN}} = 2.76$ TeV, in the low and high transverse momentum intervals $0.16 < K_{T4} < 0.3 \text{ GeV}/c$ and $0.3 < K_{T4} < 1 \text{ GeV}/c$, respectively. As in Fig. 1, the triangle and circle symbols refer to completely chaotic and partially coherent sources, respectively, in the AMPT model, and solid circles denote experimental data [10]. Fig. 3 shows the four-pion correlation functions $a_4(Q_4)$ and $b_4(Q_4)$ for the completely chaotic and partially coherent sources in the AMPT model and the experimental data in Pb-Pb central collisions at $\sqrt{s_{NN}} = 2.76$ TeV [10], where symbol meanings are the same as in Figs. 1 and 2.

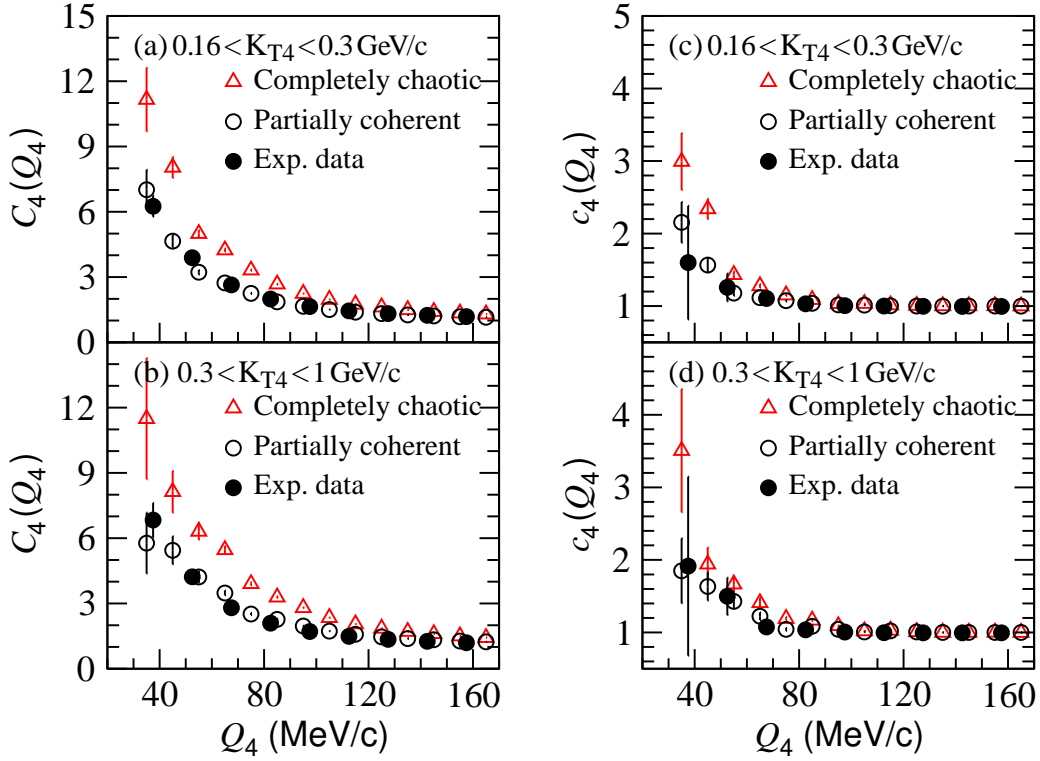


FIG. 2: (Color online) Four-pion correlation functions $C_4(Q_4)$ and $c_4(Q_4)$ for completely chaotic sources and partially coherent sources, respectively, in Pb-Pb central collisions at $\sqrt{s_{NN}} = 2.76$ TeV, calculated with the AMPT model. Experimental data [10] are plotted for comparison. Upper and Lower panels are respective results in transverse momentum intervals $0.16 < K_{T4} < 0.3$ GeV/ c and $0.3 < K_{T4} < 1$ GeV/ c .

From Figs. 1, 2, and 3, one can see that the three- and four-pion correlation functions with various cumulants for partially coherent sources in the AMPT model are all consistent with the experimental data in Pb-Pb central collisions at $\sqrt{s_{NN}} = 2.76$ TeV [10]. However, the results of the three- and four-pion correlation functions for completely chaotic sources are higher than the experimental data [10]. This consistency that all of the multi-pion correlation functions with experimental data may indicate that the partially coherent sources constructed in the AMPT model describe well the emission coherence of identical pions in the heavy-ion collisions.

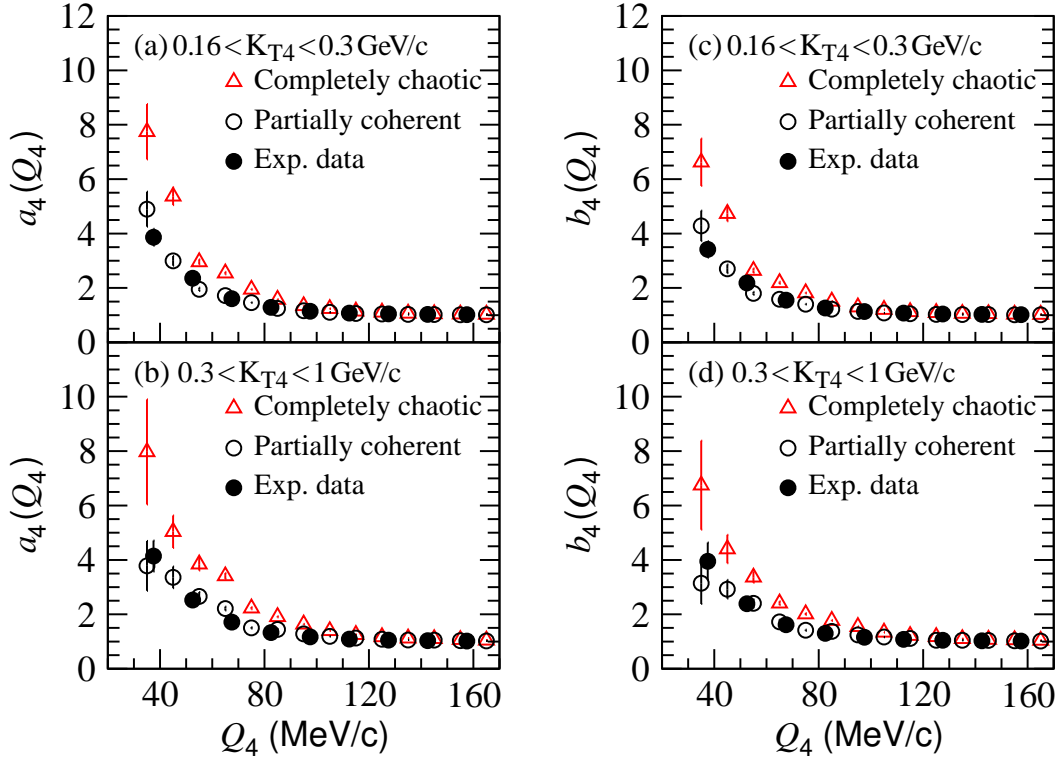


FIG. 3: (Color online) Four-pion correlation functions $a_4(Q_4)$ and $b_4(Q_4)$ for completely chaotic and partially coherent sources, respectively, in Pb-Pb central collisions at $\sqrt{s_{NN}} = 2.76$ TeV, calculated with the AMPT model. Experimental data [10] are plotted for comparison. Upper and lower panels are respective results in transverse momentum intervals $0.16 < K_{T4} < 0.3$ GeV/c and $0.3 < K_{T4} < 1$ GeV/c.

B. Multi-kaon correlation functions

In Eqs. (14) and (15), a'_Z and a'_T are considered as two universal constant parameters related only to the collision systems. They are determined in subsection III A to be 0.0031 fm and 0.662 fm², respectively, by comparing the model results with experimental data of three- and four-pion correlation functions. We assume here that these parameter values are also suitable for the kaon sources in the collisions, and investigate the three- and four-kaon correlation functions in Pb-Pb central collisions at $\sqrt{s_{NN}} = 2.76$ TeV in the AMPT model.

Figure 4 shows the three-kaon correlation functions $C_3(Q_3)$ and $c_3(Q_3)$ in Pb-Pb central collisions at $\sqrt{s_{NN}} = 2.76$ TeV, in low and high transverse momentum intervals $0.16 < K_{T3} < 0.4$ GeV/c and $0.4 < K_{T3} < 1$ GeV/c, respectively. Triangle and circle symbols, respectively, are for completely chaotic and partially coherent sources in the AMPT model. We take the

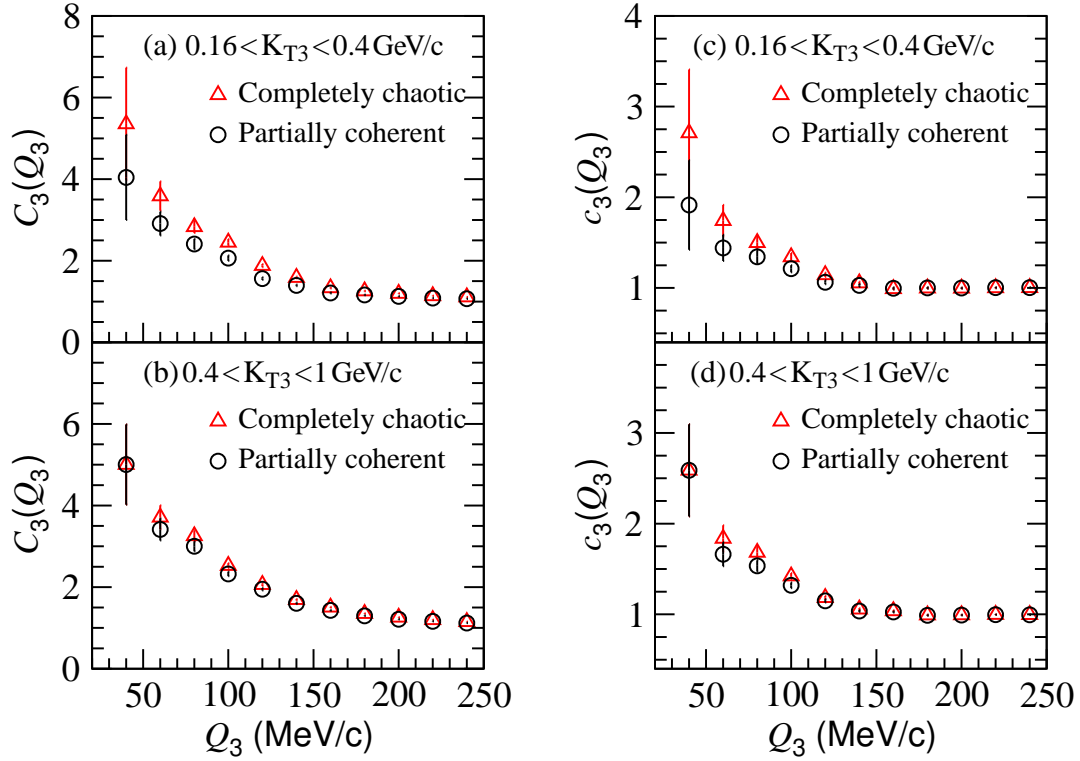


FIG. 4: (Color online) Three-kaon correlation functions $C_3(Q_3)$ and $c_3(Q_3)$ for completely chaotic and partially coherent sources, respectively, in Pb-Pb central collisions at $\sqrt{s_{NN}} = 2.76$ TeV, calculated with the AMPT model. Upper and lower panels, respectively, are results in transverse momentum intervals $0.16 < K_{T3} < 0.4$ GeV/ c and $0.4 < K_{T3} < 1$ GeV/ c .

kaon sample with the same pseudorapidity and transverse momentum cuts $|\eta| < 0.8$ and $0.16 < p_T < 1.0$ GeV/ c as in pion sample [10] for comparison. The total event number for the multi-kaon correlation calculations is 4×10^4 . One can see that the kaon correlation functions are wider than those of the pion (see Fig. 1), because the kaon source sizes are smaller. The differences between the kaon correlation functions of the completely chaotic and partially coherent sources are smaller than those of the pion sources. This means the kaon sources having lower coherence than the pion sources.

Figure 5 shows the four-kaon correlation functions $C_4(Q_4)$ and $c_4(Q_4)$, and Figure 6 shows the four-kaon correlation functions $a_4(Q_4)$ and $b_4(Q_4)$ in Pb-Pb central collisions, at $\sqrt{s_{NN}} = 2.76$ TeV. It can be seen that the differences of $C_4(Q_4)$, $a_4(Q_4)$, and $b_4(Q_4)$ between the completely chaotic and partially coherent sources in the lower K_{T4} interval are

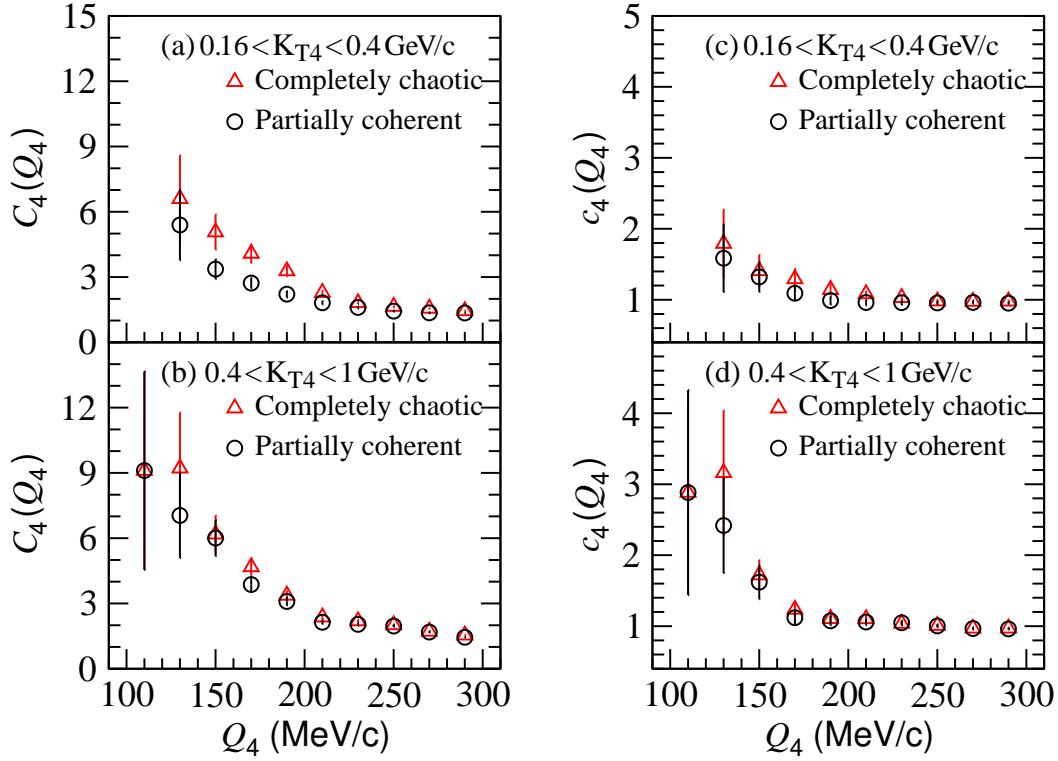


FIG. 5: (Color online) Four-kaon correlation functions $C_4(Q_4)$ and $c_4(Q_4)$ for completely chaotic and partially coherent sources, respectively, in Pb-Pb central collisions at $\sqrt{s_{NN}} = 2.76$ TeV, calculated with the AMPT model. Upper and lower panels are results in transverse momentum intervals $0.16 < K_{T4} < 0.4$ GeV/ c and $0.4 < K_{T4} < 1$ GeV/ c , respectively.

greater than those in the higher K_{T4} interval. The data at the smallest Q_4 in the higher K_{T4} interval are from the contributions of the sampled four kaons with small angles among their transverse momenta.

C. Multiboson correlation function intercepts and equivalent coherence parameters of partially coherent sources

In this study, we introduce the longitudinal and transverse coherent-emission lengths to construct the partially coherent sources of identical bosons in the AMPT model. These two coherent-emission lengths are particle momentum and density dependent. To investigate the influence of coherent emission on multi-boson HBT correlations, we introduce the intercept parameters of the three- and four-boson correlation functions λ_3 and λ_4 , respectively, and write the pure three- and four-boson correlation functions for the partially coherent sources

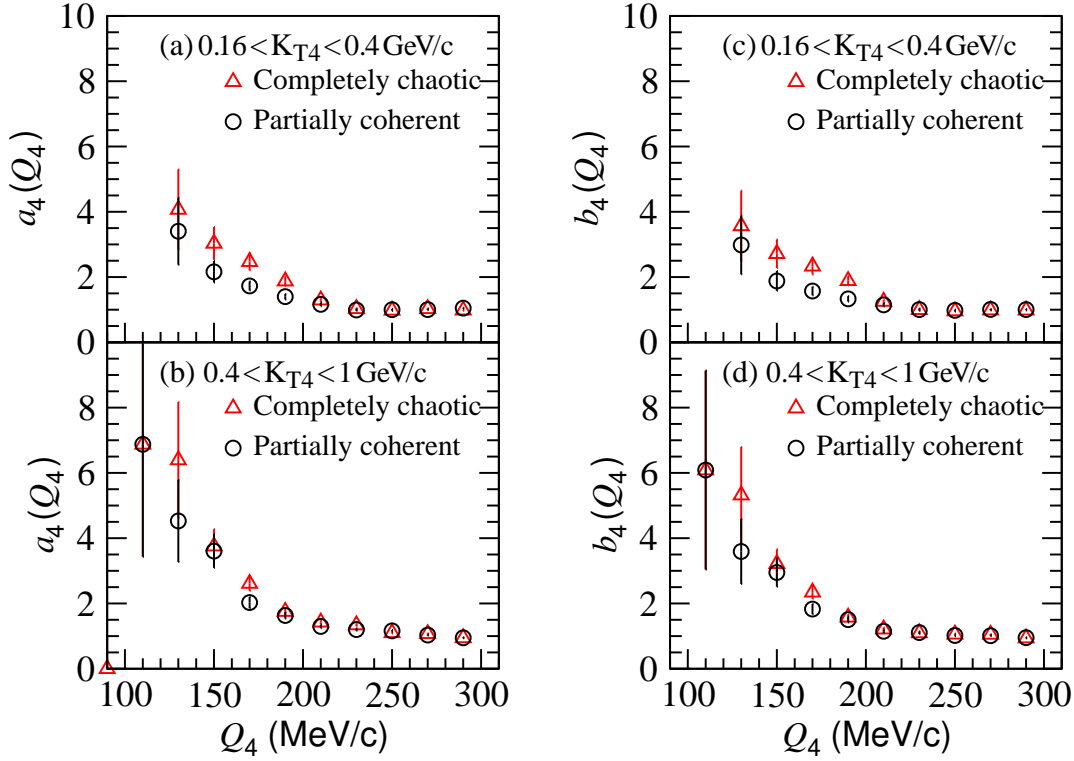


FIG. 6: (Color online) Four-kaon correlation functions $a_4(Q_4)$ and $b_4(Q_4)$ for completely chaotic and partially coherent sources, respectively, in Pb-Pb central collisions at $\sqrt{s_{NN}} = 2.76$ TeV, calculated with the AMPT model. Upper and lower panels are results in transverse momentum intervals $0.16 < K_{T4} < 0.4$ GeV/c and $0.4 < K_{T4} < 1$ GeV/c, respectively.

as

$$c_3(\mathbf{p}_1, \mathbf{p}_2, \mathbf{p}_3) = 1 + \lambda_3 R_3(\mathbf{p}_1, \mathbf{p}_2, \mathbf{p}_3), \quad (21)$$

$$c_4(\mathbf{p}_1, \mathbf{p}_2, \mathbf{p}_3, \mathbf{p}_4) = 1 + \lambda_4 R_4(\mathbf{p}_1, \mathbf{p}_2, \mathbf{p}_3, \mathbf{p}_4), \quad (22)$$

where $R_3(\mathbf{p}_1, \mathbf{p}_2, \mathbf{p}_3)$ and $R_4(\mathbf{p}_1, \mathbf{p}_2, \mathbf{p}_3, \mathbf{p}_4)$ are pure three- and four-boson correlators, respectively, which are functions of the respective relative momenta Q_3 and Q_4 . At $Q_3 = 0$ and $Q_4 = 0$, we have $\lambda_3 = 2$ and $\lambda_4 = 6$ for completely chaotic sources and $\lambda_3 = \lambda_4 = 0$ for completely coherent sources [see Eqs. (9) and (10)]. Because of the absence of sufficient statistics of the correlators near zero relative momenta Q_3 and Q_4 , it is hard to extract the intercepts directly from the correlation function data.

Based on our calculations for the correlation functions of the partially coherent sources

in the AMPT model, the intercepts can be written as

$$\lambda_3 = 2 \frac{n_{3\chi}}{n_{3t}}, \quad \lambda_4 = 6 \frac{n_{4\chi}}{n_{4t}}, \quad (23)$$

where $n_{3\chi}$ is the number of the boson triplets in which all pairs satisfied $F(\mathbf{p}_i - \mathbf{p}_j, X) = f(\mathbf{p}_i - \mathbf{p}_j, X)$ ($i, j = 1, 2, 3, i \neq j$) in Eq. (13) in the three-boson samples, $n_{4\chi}$ is the number of the boson quadruplets in which all pairs satisfied $F(\mathbf{p}_i - \mathbf{p}_j, X) = f(\mathbf{p}_i - \mathbf{p}_j, X)$ ($i, j = 1, 2, 3, 4, i \neq j$) in Eq. (13) in the four-boson samples, and n_{3t} and n_{4t} are the total numbers of the three- and four-boson samples, respectively.

For a static partially coherent boson-emitting source with the same Gaussian spatial distribution for chaotic and coherent emissions and a constant ratio γ of the coherent emission contribution b_c to the chaotic emission contribution b_χ [$\gamma = (b_c/b_\chi)$], one has with the diagram technique [20]

$$c_3(\mathbf{p}_1, \mathbf{p}_2, \mathbf{p}_3) = 1 + 2\xi_G e^{-(q_{12}^2 + q_{13}^2 + q_{23}^2)R^2/2}, \quad (24)$$

$$c_4(\mathbf{p}_1, \mathbf{p}_2, \mathbf{p}_3, \mathbf{p}_4) = 1 + 2\eta_G \left[e^{-(q_{12}^2 + q_{23}^2 + q_{34}^2 + q_{41}^2)R^2/2} + e^{-(q_{12}^2 + q_{24}^2 + q_{43}^2 + q_{31}^2)R^2/2} + e^{-(q_{13}^2 + q_{32}^2 + q_{24}^2 + q_{41}^2)R^2/2} \right], \quad (25)$$

where, $q_{ij} = |\mathbf{p}_i - \mathbf{p}_j|$ ($i, j = 1, 2, 3, 4$), R is the standard variance of the Gaussian distribution, and

$$\xi_G = \frac{1 + 3\gamma}{(1 + \gamma)^3}, \quad \eta_G = \frac{1 + 4\gamma}{(1 + \gamma)^4}. \quad (26)$$

Letting $\lambda_3 = 2\xi_G$ and $\lambda_4 = 6\eta_G$, we can obtain the equivalent coherent fractions, $CF_m = b_c/(b_c + b_\chi)$, $m = 3, 4$, with intercepts λ_3 and λ_4 for the partially coherent sources in the AMPT model. The values of equivalent coherent fractions CF_m ($m = 2, 3, 4$) provide another description of the source coherence.

Table II presents the intercept values of pion and kaon multi-particle correlation functions in the low and high transverse momentum intervals for partially coherent sources in Pb-Pb central collisions at $\sqrt{s_{NN}} = 2.76$ TeV/ c in the AMPT model. The statistical errors of the intercepts are proportional to $(n_\chi^{-1/2} + n_t^{-1/2})$, which are insignificant for large n_χ and n_t . The corresponding CF results are also presented in Table II.

It can be seen from Table II that the intercepts of the multi-pion and multi-kaon correlation functions of the partially coherent sources are higher in the high transverse momentum

TABLE II: Intercepts of multi-boson correlation functions (λ_3, λ_4) and equivalent coherent fractions (CF_3, CF_4) for partially coherent sources in Pb-Pb central collisions at $\sqrt{s_{NN}} = 2.76$ TeV in the AMPT model.

Pb-Pb@2.76 TeV	λ_3	CF_3	λ_4	CF_4
$\pi, 0.16 < K_{Tm} < 0.3 \text{ GeV/c}$	0.851	0.550	2.049	0.481
$\pi, 0.3 < K_{Tm} < 1.0 \text{ GeV/c}$	0.934	0.522	2.335	0.451
$K, 0.16 < K_{Tm} < 0.4 \text{ GeV/c}$	1.409	0.360	5.720	0.094
$K, 0.4 < K_{Tm} < 1.0 \text{ GeV/c}$	1.740	0.226	5.751	0.088

intervals than those in the low transverse momentum intervals, and similarly the equivalent coherent fractions are smaller. This is because the particle transverse de Broglie wavelengths are small at high transverse momenta. The intercept results of multi-kaon correlation functions are larger than those of multi-pion correlation functions because the kaon densities are less than the pion densities (see table I). The inconformity of the equivalent coherent fraction CF_3 with CF_4 occurs because the partially coherent sources in the AMPT model are different from those of the static Gaussian model.

IV. SUMMARY AND CONCLUSION

In this study, we investigated multi-pion and multi-kaon HBT correlations for partially coherent and completely chaotic sources in Pb-Pb central collisions at $\sqrt{s_{NN}} = 2.76$ TeV in the AMPT model. The longitudinal and transverse coherent emission lengths of the partially coherent sources are proportional to the boson de Broglie wavelengths as well as to the boson densities, and the proportionality coefficients are assumed to be universal constants both for pion and kaon partially coherent particle-emitting sources. We calculated the intercepts of the multi-pion and multi-kaon correlation functions of the partially coherent sources in the AMPT model, and investigated the influence of boson coherent emission on multi-boson HBT correlations.

It was found that the multi-boson correlation functions of partially coherent sources were lower than those of completely chaotic sources. All of the three- and four-pion correlation

functions of the partially coherent sources are consistent with experimental data. This consistency may indicate that the partially coherent source constructed in the AMPT model well describes the emission coherence of identical pions in heavy-ion collisions. Multi-kaon correlation functions are wider than multi-pion correlation functions because the kaon sources are smaller than pion sources. The intercepts of multi-boson correlation functions exhibit the influence of the source coherence on HBT correlations for partially coherent sources. The intercepts of the three- and four-kaon correlation functions of partially coherent sources are greater than those of three- and four-pion correlation functions, because low kaon densities lead to the smaller kaon coherent-emission lengths than the pion coherent-emission lengths. The intercepts of multi-pion and multi-kaon correlation functions of partially coherent sources in high transverse momentum intervals are higher than those in low transverse momentum intervals, because particle de Broglie wavelengths are small at high momenta. Our study also indicates that the partially coherent sources constructed in the AMPT model are different from those of a static Gaussian model. In this work, the coherent emissions in longitudinal and transverse directions are independent and have sharp boundaries. In future work, investigating their relation and considering more realistic coherent emission regions, for instance, with Gaussian distributions, are of interest. In addition, an investigation of two- and multi-boson HBT correlations for more collision systems in microscopic cascade models will be of interest.

Acknowledgments

We thank Zi-Wei Lin for useful discussions and suggestions. This research was supported by the National Natural Science Foundation of China under Grant No. 12175031. We thank LetPub (www.letpub.com.cn) for its linguistic assistance during the preparation of this manuscript.

-
- [1] M. Gyulassy, S. K. Kauffmann, and Lance W. Wilson, Phys. Rev. C **20**, 2267 (1979).
 - [2] C. Y. Wong, *Introduction to High-Energy Heavy-Ion Collisions* (World Scientific, Singapore, 1994), Chap. 17.
 - [3] U. A. Wienemann and U. Heinz, Phys. Rep. **319**, 145 (1999).

- [4] R. M. Weiner, Phys. Rep. **327**, 249 (2000).
- [5] T. Csörgő, Heavy Ion Physics **15** (2002) 1; arXiv:hep-ph/0001233.
- [6] M. A. Lisa, S. Pratt, R. Soltz, and U. Wiedemann, Annu. Rev. Nucl. Part. Sci. **55**, 357 (2005).
- [7] B. Abelev *et al.* (ALICE Collaboration), Phys. Rev. C **88**, 044910 (2013).
- [8] B. Abelev *et al.* (ALICE Collaboration), Phys. Lett. B **739**, 139 (2014).
- [9] B. Abelev *et al.* (ALICE Collaboration), Phys. Rev. C **89**, 024911 (2014).
- [10] J. Adam *et al.* (ALICE Collaboration), Phys. Rev. C **93**, 054908 (2016).
- [11] D. Gangadharan, Phys. Rev. C **92** 014902 (2015).
- [12] G. Bary, P. Ru, and W. N. Zhang, J. Phys. G **45** 065102 (2018).
- [13] G. Bary, P. Ru, and W. N. Zhang, J. Phys. G **46** 115107 (2019).
- [14] G. Bary, W. N. Zhang, P. Ru, and Jing Yang, Chin. Phys. C **45** 024106 (2021).
- [15] C. Adler *et al.* (STAR Collaboration), Phys. Rev. Lett. **87**, 082301 (2001).
- [16] S. S. Adler *et al.* (PHENIX Collaboration), Phys. Rev. Lett. **93**, 152302 (2004).
- [17] J. Adams *et al.* (STAR Collaboration), Phys. Rev. C **71**, 044906 (2005).
- [18] B. I. Abelev *et al.* (STAR Collaboration), Phys. Rev. C **81**, 024911 (2010).
- [19] J. Adam *et al.* (ALICE Collaboration), Phys. Rev. C **92**, 054908 (2015).
- [20] Y. M. Liu, D. Beavis, S. Y. Chu, S. Y. Fung, D. Keane, G. VanDalen, and M. Vient, Phys. Rev. C **34** 1667 (1986).
- [21] U. Heinz and Q. H. Zhang, Phys. Rev. C **56** 426 (1997).
- [22] U. Heinz and A. Sugarbaker, Phys. Rev. C **70** 054908 (2004).
- [23] Z. W. Lin and C. M. Ko, Phys. Rev. C **65**, 034904 (2002).
- [24] Z. W. Lin, C. M. Ko, B. A. Li, B. Zhang, and S. Pal, Phys. Rev. C **72**, 064901 (2005).
- [25] S. Y. Wang, J. T. Ye, and W. N. Zhang, Phys. Rev. C **109**, 014912 (2024).
- [26] Z. W. Lin and C. M. Ko, J. Phys. G **30**, S263 (2004).
- [27] M. Nasim, L. Kumar, P. Kumar, and B. Mohanty, Phys. Rev. C **82**, 054908 (2010).
- [28] J. Xu and C. M. Ko, Phys. Rev. C **83**, 021903(R) (2011).
- [29] D. Solanki, P. Sorensen, S. Basu, R. Raniwala and T. K. Nayak, Phys. Lett. B **720**, 352 (2013).
- [30] Y. L. Xie, G. Chen, J. L. Wang, Z. H. Liu and M. J. Mang, Nucl. Phys. A **920**, 33 (2013).
- [31] A. Bzdak and G. L. Ma, Phys. Rev. Lett. **113**, 252301 (2014).
- [32] G. L. Ma and Z. W. Lin, Phys. Rev. C **93**, 054911 (2016).

- [33] H. Li, L. He, Z. W. Lin, D. Molnar, F. Wang, and W. Xie, Phys. Rev. C **96**, 014901 (2017).
- [34] M. R. Haque, M. Nasim, and B. Mohanty, J. Phys. G **46**, 085104 (2019).
- [35] M. Dordevic, J. Milosevic, L. Nadder, M. Stojanovic, F. Wang, and X. Zhu, Phys. Rev. C **101**, 014908 (2020).
- [36] T. Shao, J. Chen, C. M. Ko, and Z. W. Lin, Phys. Rev. C **102**, 014906 (2020).
- [37] K. J. Sun and C. M. Ko, Phys. Rev. C **103**, 064909 (2020).
- [38] N. Magdy and R. A. Lacey, Phys. Rev. C **104**, 014907 (2021).
- [39] S. Basu, V. Gonzalez, J. Pan, A. Knospe, A. Marin, C. Markert, C. Pruneau, Phys. Rev. C **104**, 064902 (2021).
- [40] N. Magdy, O. Evdokimov, and R. A. Lacey, J. Phys. G **48**, 025101 (2021).
- [41] Z. Zhang, N. Yu, and H. Xu, Eur. Phys. J. A **58**, 240 (2022).
- [42] X. N. Wang and M. Gyulassy, Phys. Rev. D **44**, 3501 (1991).
- [43] B. Zhang, Comput. Phys. Commun. **109**, 193 (1998).
- [44] B. A. Li and C. M. Ko, Phys. Rev. C **52**, 2037 (1995).
- [45] B. Abelev *et al.* (ALICE Collaboration), Phys. Rev. C **88**, 044909 (2013).